# Design and fabrication of micro and nano-structured scaffolding biomaterials for tissue engineering applications *via* low temperature supercritical $CO_2$ processes

A. Salerno[1,2,3,*], P.A. Netti[3], C.A. García-González[1], C. Domingo[1,*]
[1]*Instituto de Ciencia de Materiales de Barcelona (ICMAB-CSIC), Campus de la UAB s/n, Bellaterra, Spain. E-mail: conchi@icmab.es*
[2]*Institute of Composite and Biomedical Materials, National Research Council (IMCB-CNR), Piazz.le Tecchio 80, Naples, Italy. E-mail: asalerno@unina.it*
[3] *Center for Advanced Biomaterials for Healthcare (IIT-CRIB), Piazz.le Tecchio 80, 80125 Naples, Italy*

## ABSTRACT

In designing novel scaffolding biomaterials for tissue engineering (TE) strategies, one of the most challenging goals is the design of three-dimensional porous architectures with well controlled pore size and shape distributions, as well as appropriate pore interconnectivity and nano and micro-metric topographical features. Supercritical $CO_2$ ($scCO_2$) has achieved great emphasis in TE because it may allow to produce porous biomaterial scaffolds avoiding the use of organic solvents, potentially harmful to cells and bioactive molecules. Although great advances have been achieved along this research field, to date the great potential of this technology has not been satisfactory explored and, further efforts are strongly required for the production of novel biomaterial scaffolds for TE applications.

In the present work we reported the design and fabrication of novel biomaterial scaffolds for TE by using the $scCO_2$ technology. Two different processes were used to achieve this aim: (i) the solid-state $scCO_2$ foaming, and (ii) the antisolvent $scCO_2$ precipitation. In particular, the first technique was optimized aiming to produce three-dimensional interconnected porous scaffolds with a micro-metric bi-modal pore size distribution. This was achieved by the optimization of the composition and thermal history of the materials and, by the control of the depressurization profile during foaming. Furthermore, a $scCO_2$ antisolvent technique was implemented in order to produce porous biocompatible scaffolds with fibrous morphology and nano-metric architecture. To this purpose, the composition of the starting solution, in terms of polymer and inorganic filler type and concentration, as well as processing conditions, were accurately selected to control the precipitation of the biomaterials and, therefore, the final properties of the scaffolds. The results of this study demonstrated that the proposed $scCO_2$ processes may be successfully used in order to produce porous biomaterial scaffolds with micro and nano-structured architectures suitable for TE applications.

## INTRODUCTION

Tissue engineering is evolving from the use of implants that repair or replace damaged parts, to the use of controlled three-dimensional scaffolds that induce the formation of new functional tissues either *in vitro or in vivo*. Many polymeric scaffolds are being evaluated for a possible role in tissue engineering. Biodegradable homopolymers and copolymers of lactic (L-PLA) and glycolic (PGA) acids are typically chosen for these applications. Poly(ε-

caprolactone) (PCL), had also attracted attention as a biopolymer due to the lack of toxicity and low cost, although it is a slow degradation polymer. Non-biodegradable materials such as polymethylmethacrylate (PMMA) are being also tested in tissue engineering to achieve long-term mechanical stability after implantation. Along with the ongoing search for new materials, polymeric blends composed by a biostable polymer and a biodegradable one have recently gained significant attention in tissue engineering due to the possibility of provide them with specific advantages in morphological, degradation and mechanical properties. Not only the chemical composition, but also the architecture of a scaffold plays an important role in modulating tissue growth and response behavior of cultured cells. Required characteristics include high porosity and an interconnected 3D macroporous network necessary for cell proliferation, and high surface area to promote cell adhesion. Scaffolds can take forms ranging from complex monolithic 3D microcellular structures (macroporous sponges) to networks of fibers.

Scaffolds can be produced in a variety of ways, using either conventional techniques such as solvent casting, foaming, physical separation and freeze drying or advanced processing methods such as rapid prototyping technologies. The main drawbacks of conventional scaffolds production methods involve a reduced capability to control pore size and pore interconnectivity. Moreover, when using solvent approaches, the residual organic molecules left in the polymer after processing may be harmful to the transplanted cells and can inactivate biologically active growth factors. Technology based on supercritical carbon dioxide ($scCO_2$) is an alternative to overcome some of the problems associated with the use of traditional organic solvents for pharmaceuticals and biomaterials preparation. $scCO_2$ is used to produce polymer foams by pressure-induced phase separation [1-3]. Furthermore, spray processes involving $SCCO_2$ have achieved considerable success in addressing polymer particles and fibers production [4-7]. $SCCO_2$ was used in this work for the preparation of foamed sponges and intermingled fibers of several polymers.

## EXPERIMENTAL

### Materials

The used polymers are shown in Table 1. Dichloromethane (DCM HPLC grade, Prolabo) and $CO_2$ (99.5 wt %, Air Liquide) were the used fluids. HA nano-particles (Berkeley Advanced Biomaterials Inc., Berkeley, CA) with 100 nm mean size were selected for the preparation of the PCL-HA composites.

**Table 1**. Characteristics of polymers employed.

| Sample | Polymer | Supplier | Molecular weight [$gmol^{-1}$] | Structure | Thermal transitions [K] |
|---|---|---|---|---|---|
| $PLA_{Bio}$ | L-PLA | Biovalley | 100 000 | semicrystalline | $T_g = 320$<br>$T_m = 449$ |
| $PCL_{Ald}$ | PCL | Aldrich | 14 000 | semicrystalline | $T_g = 211$<br>$T_m = 339$ |
| $PCL_{Ald}$ | PCL | Aldrich | 45 000 | semicrystalline | $T_g = 211$<br>$T_m = 339$ |
| $PMMA_{BP}$ | PMMA beads | Bonar Polymers | 300 000 | amorphous | $T_g = 393$ |

**Experimental set up**

The experimental tests were carried out with two objectives, either the production of monolithic foams or the precipitation of fibers.

***Solid foams production:*** A PCL-HA nano-composite containing 5 wt% of inorganic particles was prepared by using an internal mixer (Rheomix® 600, Haake, Germany) controlled by a measuring drive unit (Rheocord® 9000, Haake, Germany). PCL pellets were first melted and, subsequently, the HA particles were added into the mixing chamber and mixed with the polymer at 70°C, 100 rpm for 10 min. The as obtained sample was extracted from the mixer and compression moulded to produce 200 µm-thick films, by a hot press (P 300 P, Collin, Germany) at 80°C and at 10 MPa. Three different cooling histories were used to cool down the molten samples from 80 to 25°C: (1) the molten material was quenched by soaking in liquid N2 (fast cooling rate); within the press, the material was allowed to cool to room temperature in (2) 2 minutes (intermediate cooling rate) and (3) 15 minutes (slow cooling rate). Neat PCL was subjected to the same processes for proper comparison. All of the samples were then stored at -30ºC to avoid polymer re-crystallization before further processing. Foaming experiments were carried out on disc-shaped samples obtained by overlapping five samples (200 µm-thick and 10 mm in diameter) characterized by the same composition and thermal history. The solubilisation of the $scCO_2$ was performed at saturation pressures and temperatures in the range from 10 to 20 MPa and from 37 to 40°C, respectively, while the solubilisation time was varied from 1.5 to 12 hours. Foaming was induced by quenching the pressure to the ambient. Three different foaming times, in the range from 2 to 900 s and obtained by selecting different gas-discharge capillaries with appropriate length and diameter of the $scCO_2$ release system, were used to control the pore structure features of the foams

***Semicontinuous equipment:*** The PCA experiments were conducted in the apparatus shown schematically in Fig. 1, operated in a semi-continuous mode. The spray chamber consisted on a high pressure vessel (Autoclave Engineers) of 5 cm i.d. x 25 cm long. Dichloromethane solutions of polymer were sprayed into the precipitation chamber using a minipump (Milton Roy LDC). In a typical experiment, once the temperature of the vessel had attained the desired value (313 K), the $CO_2$ was introduced until the desired pressure was reached (11 MPa). Then, valve (V) was opened and the system was allowed to equilibrate maintaining the $CO_2$ flow at a fixed value (ca. 100 $mLmin^{-1}$). The polymer solution was introduced into the precipitation chamber through a nozzle and the $CO_2$ through a 1/8” tubing.

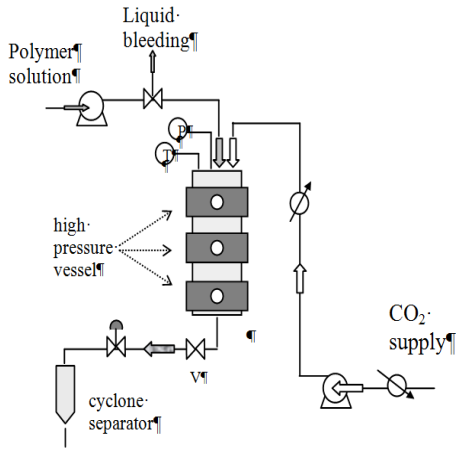


**Figure 1.** Experimental apparatus used for PCA experiments.

**Characterization**

The differential scanning calorimetry (DSC) was used to assess the effect of the thermal history and scCO2 solubilization on the melting properties of PCL and PCL-HA nano-composite. The morphology of the samples was assessed by scanning electron microscopy (SEM). The samples were cross-sectioned, gold sputtered and analyzed by SEM (S440, LEICA, Germany).

The density of the foams ($\rho_F$) was determined from the mass and the volume measurements. The mass was measured by using a high accuracy balance ($10^{-4}$ g, AB104-S, Mettler Toledo, Italy) while the volume determined by displacement method (ASTM D1622-03). The porosity of the foams was then assessed by the following equation [3]:

$$\text{Porosity } \% = [1-(\rho_F/\rho_P)] * 100$$

where $\rho_P$ is the density of the polymeric phase (pure PCL or PCL-HA composite).

The mean pore size and the pore size distribution of the foams were evaluated by image analysis. One hundred pores for each sample were analyzed by using the ‘‘particle analysis’’ tools of the Image J software pack, that enable to assess the area of each pores. The pore diameter was then calculated with the hypothesis of spherical shape pores and, by correcting the as obtained values by the factor $4/\pi$, according to the ASTM D3576.

The number of pores per $cm^3$ of the foam ($N_f$) was assessed by using the equation [1]:

$$N_f = \text{porosity} / [(\pi/6) \text{ x } (\text{pore diameter})^3]$$

**RESULTS**

Two different processes were used to fabricate scaffolds for TE: (i) the solid-state $scCO_2$ foaming, and (ii) the antisolvent $scCO_2$ precipitation. In particular, the first technique was optimized aiming to produce three-dimensional interconnected porous scaffolds with a micrometric bimodal pore size distribution.

**Microcellular foaming**

In this work we performed a systematic investigation on the material/processing/pore structure properties of PCL and PCL-HA nano-composite scaffolds prepared by the solid-state scCO2 foaming. All of the tests were performed at saturation and foaming temperatures below or equal to 40°C, which is considered suitable for possible incorporation of heat labile molecules within the scaffolds.

Figure 2 reported the morphology of PCL scaffolds as a function of the thermal history and depressurization time. As shown, all of the samples were characterized by rather homogeneous morphologies. However, significant differences were observed with respect to the different processing conditions. In particular, the pore size increased with the increase of the depressurization time, with the PCL samples prepared at the depressurization time of 900 s that were characterized by larger pores if compared to those obtained at 2 and 15 s. Although minor differences were observed on the morphology of the foams as a function of the cooling process for a depressurization time of 2 or 15 s, in the case of the depressurization time of 900 s, the pore size interestingly increased with the decrease of the cooling time (compare Figures 2g, h and i).

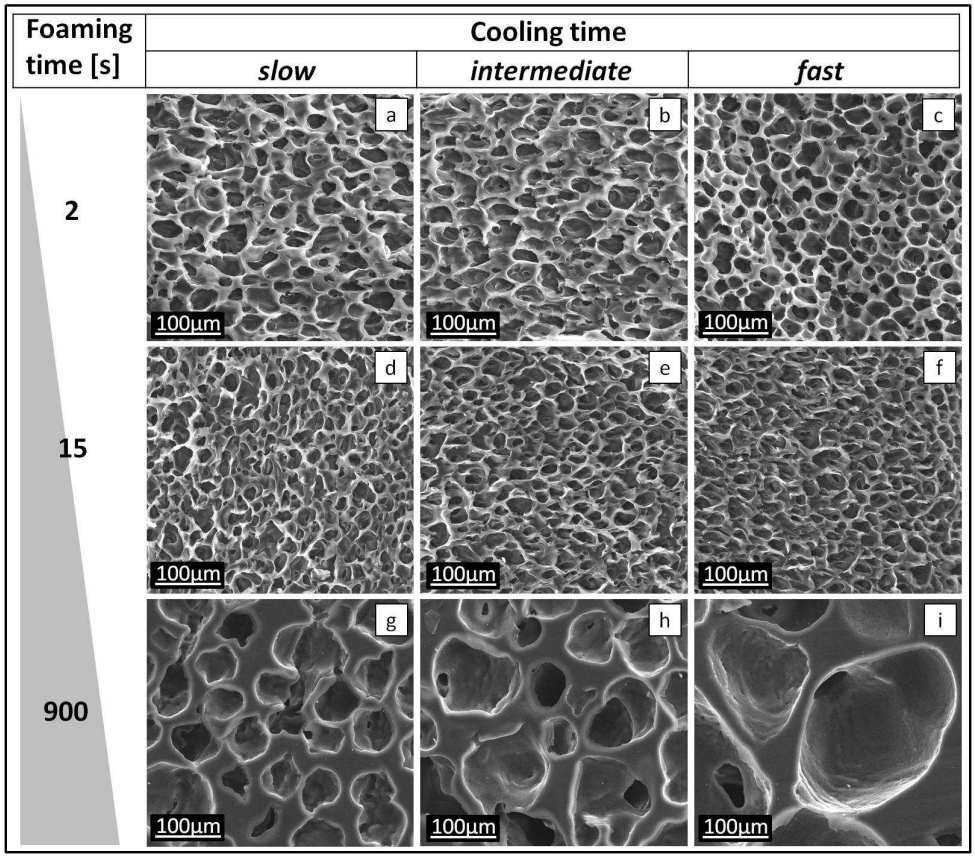


**Figure 2.** SEM microscope images of the cross-sections of the PCL scaffolds evidencing the effect of the thermal history and foaming time on the morphology of the samples. [1]

Figure 3 reports the porosities of the PCL and PCL-HA scaffolds as a function of the depressurization time and thermal history.

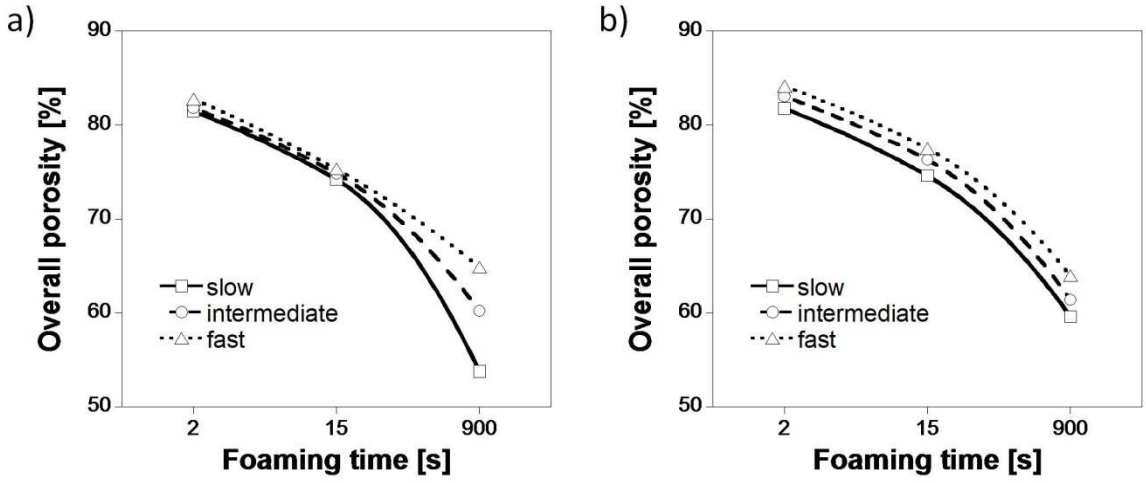


**Figure 3.** Porosity of the scaffolds as a function of the thermal history and foaming time: (a) PCL and (b) PCL-HA. [1]

In agreement with the images of Figure 2, we observed that the highest porosity value, equal to 82 %, was achieved in the case of the PCL sample prepared at a depressurization time of 2 s (Figure 3a). Lower porosity values, in the range from 55 to 65%, were conversely achieved when depressurization was performed for 900 s. The decrease of the porosity with the increase of the foaming time was more marked for the slowly cooled PCL sample, characterized by a 30% porosity decrease from 2 to 900 s of depressurization (Figure 3a). Similar results were obtained for the PCL-HA nano-composite, indicating a minor influence of the inorganic filler on the density and porosity of the foams (Figure 3b).

To evaluate the feasibility of the solid-state scCO2 foaming process to produce porous PCL and PCL-HA scaffolds with bi-modal pore size distribution and improved interconnectivity, we performed a different tests based on a two-step of depressurization. Figure 4 showed the morphology and pore size distribution of the scaffolds as a function of the intermediate pressure.

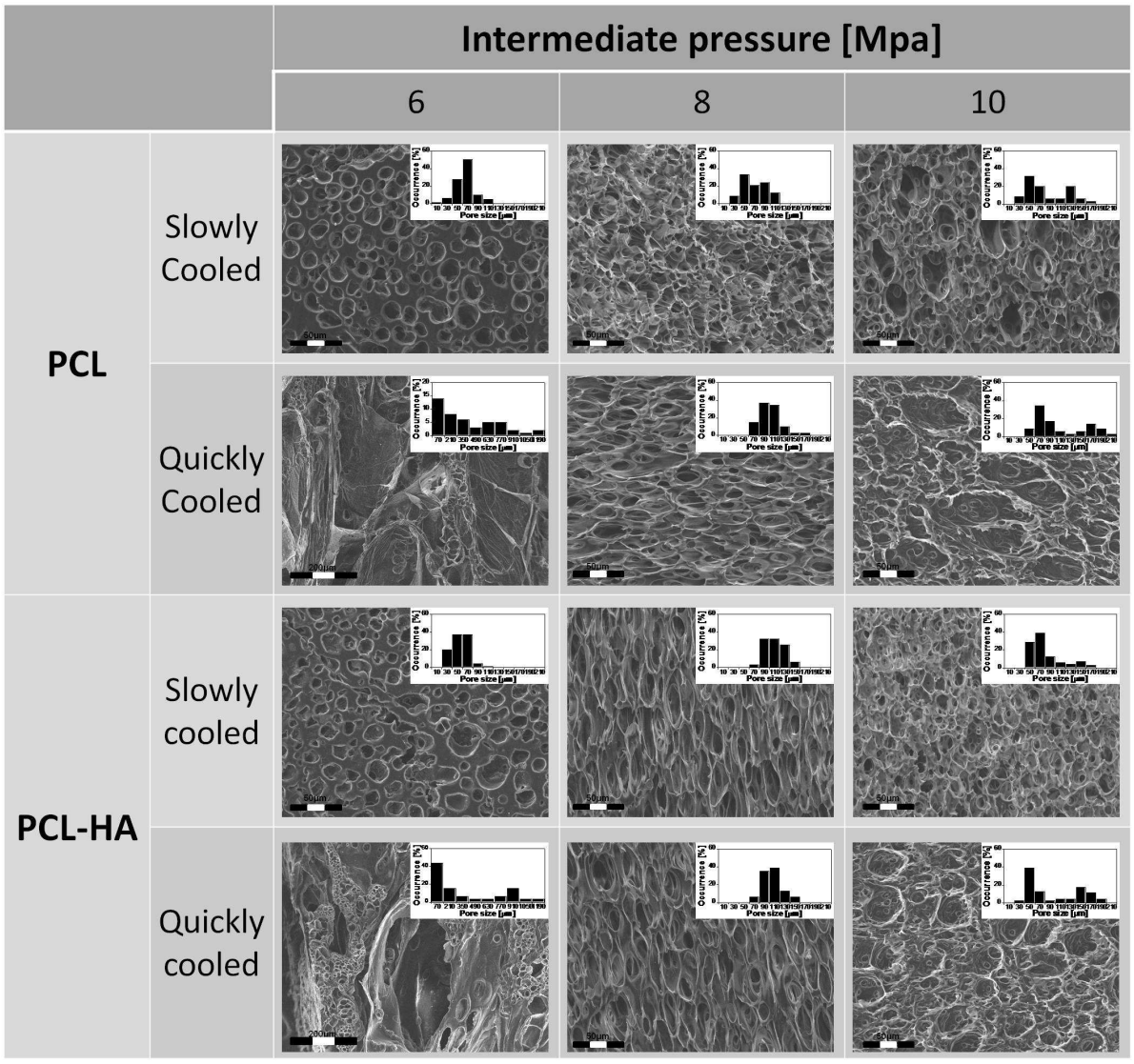


**Figure 4.** Morphology and pore size distribution of the PCL and PCL-HA nano-composite scaffolds as a function of the intermediate pressure and thermal history. [2]

The depressurization profile had a strong impact on the pore structure features of the scaffolds. In particular, at the intermediate pressure of 10 MPa, we obtained porous PCL and PCL-HA scaffolds with bi-modal pore size distributions and characterized by a macro-porosity, with pore sizes in the range from 100 to 300 µm, and a micro-porosity with mean pore size in the 50-70 µm range. Furthermore, for these samples the increase of the cooling rate resulted in the slight increase of the size and extent of the macro-porosity. When the intermediate pressure decreased down to 8 MPa, the scaffolds showed mono-modal pore size distribution and high degrees of pores interconnection. Interestingly, depending on the thermal history of the PCL and PCL-HA films, completely different pore structure features were observed at the intermediate pressure of 6 MPa. In effect, when prepared from the slowly cooled films, the PCL and PCL-HA scaffolds evidenced mono-modal pore size distributions with mean pore sizes equals to 65 ± 18 µm and 57 ± 21 µm, respectively. Conversely, the samples quenched in liquid N2 produced porous scaffolds with a bi-modal distribution of pores size and non-homogeneous morphologies. In particular, smaller pores with a mean size equal to 93 ± 28 µm for neat PCL and to 65 ± 31 µm for PCL-HA, were randomly distributed all around very large pores, characterized by mean pore sizes equals to 614 ± 269 µm and 745 ± 345 µm, respectively.

**Fibers**

The semicontinuous PCA equipment shown in Fig. 1 was used to produce fibers of various biopolymers. Basically, a homogeneous solution of the polymer to be precipitated was dissolved in dichloromethane and was sprayed through an atomization device into a continuous $scCO_2$ dense phase which played the role of the antisolvent. The simultaneous mass transfer of the dense gas and of the solvent from one phase to the other induced the supersaturation of the polymer that precipitates. A very important parameter that influences product morphology is the polymer concentration in the spraying solution. In the semidilute region, the polymer chains are capable of entangling each other strongly to form a network and a fibrous structure. PCA process was first studied for the precipitation of fibers of the homopolymers L-PLA and PMMA. Further, a PMMA/PCL blend plus a dispersed inorganic filler was also processed into fibers (Table 2).

**Table 2.** Experimental conditions for the antisolvent experiments.

| Polymer | P [MPa] & T[K] | Depres. rate [$MPas^{-1}$] | [Polymer] [%wt] | OFlow rate [$mLmin^{-1}$] | Nozzle d [µm] |
|---|---|---|---|---|---|
| $PLA_{Bio}$ | 11&313 | --- | 2.8 | 1 | disc, 100 |
| $PMMA_{BP}$ | 11&313 | --- | 1 | 1 | swirl, 100 |
| 85%$PMMA_{BP}$ 15%$PCL_{Ald}$ | 11&313 | --- | 0.8 | 1 | swirl, 100 |

***L-PLA:*** For $PLA_{Bio}$ system, polymer solutions were sprayed through a plain orifice nozzle at 1 $mLmin^{-1}$ flow rate (Table 2). Fig. 4 shows the micrographs of the obtained samples. Fibers constituted by polymer microspheres were obtaine. Coalescence of L-PLA particles seems limited to physical interaction. Indeed, the semicrystalline structure of the L-PLA made agglomeration from plasticization difficult.

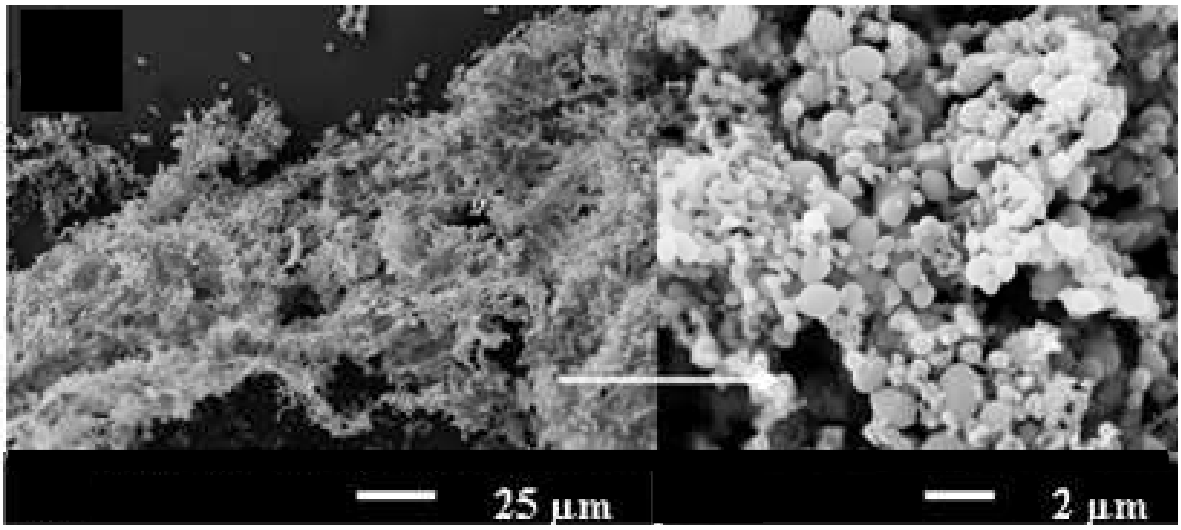


**Figure 4.** L-PLA ($PLA_{Bio}$) precipitated using the PCA process, organic phase=DCM + 2.8 %wt of polymer injected.

***PMMA:*** Under the studied experimental conditions of pressure and temperature and whatever the spray mode, $PMMA_{BP}$ polymer always precipitated as a fibrous network. SEM images in Fig. 5 show PMMA typical fibers in a network-like configuration (Table 2).

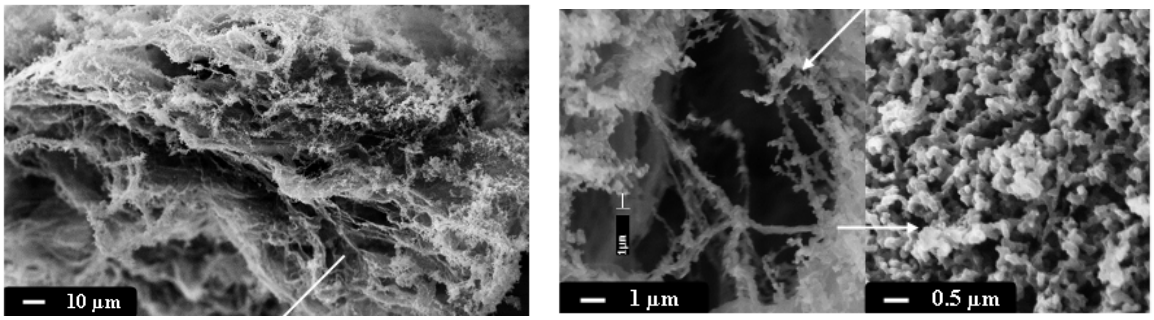


**Figure 5.** $PMMA_{BP}$ precipitate using the PCA process, organic phase=DCM + 1 %wt of polymer.

The macrostructure can be described as open airy fibers that are composed of very small subfibers of less than 0.5 µm organized in a three-dimensional network. The primary fibers are constituted of particles of *ca.* 200 nm fused end-to-end. For PMMA the agglomeration and flocculation was extended in comparison with L-PLA due to its amorphous nature and $SCCO_2$ plasticization effect.

***PMMA/PCL blend and inorganic particles:*** The PCA supercritical technique has also been used to prepare PMMA/PCL blends. Our approach to obtain a polymer blend was to precipitate the two polymers from solution rapidly with an antisolvent. The obtained precipitates had a network-like appearance similar to that obtained for raw PMMA homopolymer. A modification of the PCA technique was used to precipitate blends of PMMA/PCL loaded with silanized (hydrophobized) $TiO_2$ powder. In the used process, the inorganic filler was suspended in a solution formed by dichloromethane and the polymer. Loadings of 20 wt% of $TiO_2$ were achieved for the blend systems (Fig. 6).

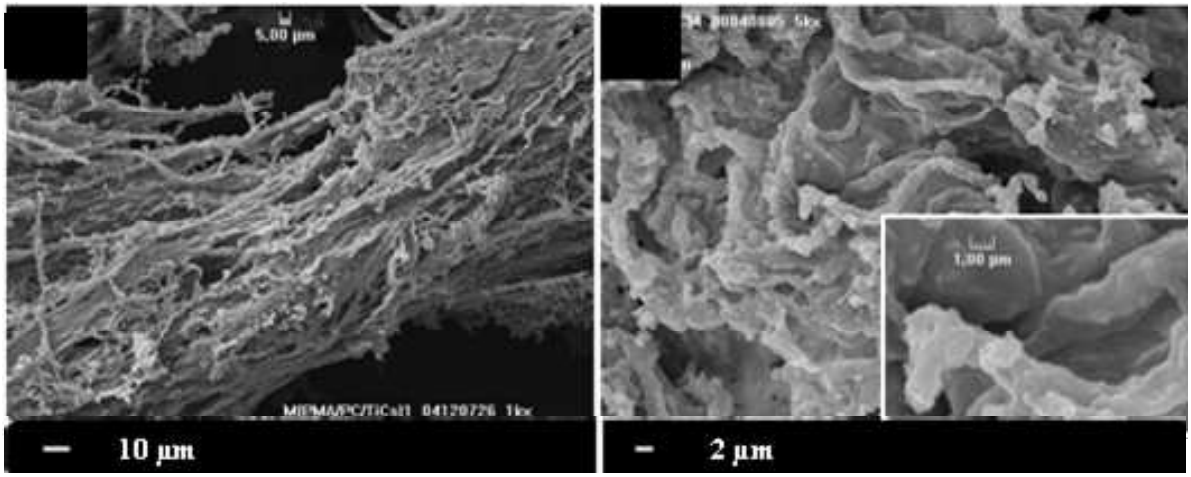


**Figure 6.** SEM pictures of precipitated fibers of PMMA/PCL and silanized $TiO_2$.

## CONCLUSIONS

The clinical success of a tissue construction is largely dependent on the quality of the starting scaffold.

The results of the foaming experiments demonstrated that the control of the thermal history and foaming parameters is essential to design scaffolds with suitable expansion ratios and homogeneous pore structures. Indeed, scaffolds with high controlled morphology, porosity and pore size distributions were achieved by selecting a saturation pressure and temperature of 20 MPa and 37ºC, respectively, and by the modulation of the depressurization time in the range from 2 to 900 s. Furthermore, we reported that the thermal history had a pivotal role on the solid-state scCO2 foaming of PCL and PCL-HA. In particular, when quenched in liquid N2, the PCL and PCL-HA produced scaffolds with higher porosity, in the range from 75 to 83%, and mean pore size, from 40 to 300 µm, if compared to those prepared from the slowly and intermediate cooled samples.

Finally, by performing a two-step depressurization foaming starting from the PCL and PCL-HA nano-composite samples quenched in liquid N2, we prepared scaffolds with bi-modal and highly interconnected porosities, therefore opening new routes for the design of porous scaffolds for TE applications.

Fibers of PMMA and L-PLA homopolymers and PMMA/PCL blend have been fabricated using the antisolvent PCA process. Topics that need further investigation are the modification of the PCA prepared fibrous networks through post-processing protocols (f.i., thermal fiber bonding) in order to improve the control in the mechanical properties of the obtained structures necessary to prove the viability of the material in tissue engineering.

## REFERENCES

[1] SALERNO, A., DI MAIO, E., IANNACE, S., NETTI, P.A., J. Super. Fluids., 58, **2011**, 158.

[2] SALERNO, A., DI MAIO, E., IANNACE, S., NETTI, P.A., Macromol. Rapid Comm., 32, **2011**, 1150.

[3] SALERNO, A., ZEPPETELLI, S., DI MAIO, E., IANNACE, S., NETTI, P.A., Comp. Sci. Tech., 70, **2010**, 1838.
[4] VEGA-GONZALEZ, A., DOMINGO, C., ELVIRA, C. and SUBRA, P., J. Appl, Polym. Sci., 91, **2004**, 2422.
[5] VEGA-GONZALEZ, A., SUBRA-PATERNAULT, P., LOPEZ-PERIAGO, A.M., GARCIA-GONZALEZ, C.A. and DOMINGO, C., Eur. Polym. J., 44, **200**8, 1081.
[6] LOPEZ-PERIAGO, A.M., VEGA, A., SUBRA, P., ARGEMÍ, A., SAURINA, J., C.A. GARCÍA-GONZÁLEZ and DOMINGO, C., J. Mater. Sci., 43, **2008**, 1939.
[7] GARCÍA-GONZÁLEZ, C.A., VEGA-GONZÁLEZ, A., LÓPEZ-PERIAGO, A.M., SUBRA-PATERNAULT, P. and DOMINGO, C., Acta Biomater., 5, **2009**, 1094.